NeuroImage 218 (2020) 116981

Contents lists available at ScienceDirect

NeuroImage

journal homepage: www.elsevier.com/locate/neuroimage

Decoding motor imagery and action planning in the early visual cortex: Overlapping but distinct neural mechanisms

Simona Monaco [a,*], Giulia Malfatti [a], Jody C. Culham [b], Luigi Cattaneo [a], Luca Turella [a]

[a] Center for Mind/Brain Sciences (CIMeC), University of Trento, 38068, Rovereto, Italy
[b] Brain and Mind Institute and Department of Psychology, University of Western Ontario, London, Ontario, N6A 5B7, Canada

ARTICLE INFO

Keywords:
Functional magnetic resonance imaging (fMRI)
Multivoxel pattern analysis (MVPA)
Humans
Action
Motor imagery
Planning
Action intention
Early visual cortex

ABSTRACT

Recent evidence points to a role of the primary visual cortex that goes beyond visual processing into high-level cognitive and motor-related functions, including action planning, even in absence of feedforward visual information. It has been proposed that, at the neural level, motor imagery is a simulation based on motor representations, and neuroimaging studies have shown overlapping and shared activity patterns for motor imagery and action execution in frontal and parietal cortices. Yet, the role of the early visual cortex in motor imagery remains unclear. Here we used multivoxel pattern analyses on functional magnetic resonance imaging (fMRI) data to examine whether the content of motor imagery and action intention can be reliably decoded from the activity patterns in the retinotopic location of the target object in the early visual cortex. Further, we investigated whether the discrimination between specific actions generalizes across imagined and intended movements. Eighteen right-handed human participants (11 females) imagined or performed delayed hand actions towards a centrally located object composed of a small shape attached on a large shape. Actions consisted of grasping the large or small shape, and reaching to the center of the object. We found that despite comparable fMRI signal amplitude for different planned and imagined movements, activity patterns in the early visual cortex, as well as dorsal premotor and anterior intraparietal cortex, accurately represented action plans and action imagery. However, movement content is similar irrespective of whether actions are actively planned or covertly imagined in parietal but not early visual or premotor cortex, suggesting a generalized motor representation only in regions that are highly specialized in object directed grasping actions and movement goals. In sum, action planning and imagery have overlapping but non identical neural mechanisms in the cortical action network.

1. Introduction

Mental imagery allows for the simulation of sensations and actions without any sensory input or motor output. While visual imagery consists of the generation of a perceptual representation of a scene or object, imagined actions rely on specific cognitive processes typically named "motor imagery" and require the visualisation of a movement without actually executing it (Bruno et al., 2018; Ehrsson et al., 2003). Motor imagery is a powerful tool with several important applications for clinical populations. Indeed, imagery is not only used as an effective approach for post-stroke rehabilitation (Page et al., 2007), but also as a control strategy for brain-computer interfaces which allow individuals with severe motor impairments to control effectors with training that consists of imagining what they want the effector to do (Green and Kalaska, 2011). In addition, in neurologically intact individuals motor imagery improves performance of acquired skills and acquisition of new ones (Annett, 1995). In fact, motor skills have been consistently shown to improve following both motor as well as mental training that involves motor imagery, and the resulting motor improvement is associated with cerebral plasticity (Doyon et al., 2003). Interestingly, motor imagery training, but not motor training, induces modifications in the early visual cortex (EVC), suggesting that motor and imagery-induced behavioural improvements rely on partly different brain mechanisms (Nyberg et al., 2006).

Abbreviations: fMRI, Functional magnetic resonance imaging; MVPA, multivoxel pattern analysis; EVC, early visual cortex; aIPS, intraparietal sulcus; M1/S1, primary motor/somatosensory cortex; dPM, dorsal premotor cortex; vPM, ventral premotor cortex; V1, primary visual cortex; LH, left hemisphere; RH, right hemisphere; ROI, region of interest; GLM, general linear model; FDR, false discovery rate; MT, movement time; RT, reaction time.

* Corresponding author. Via delle Regole 101, 30123, Trento, Italy.
E-mail address: simona.monaco@gmail.com (S. Monaco).

https://doi.org/10.1016/j.neuroimage.2020.116981
Received 23 December 2019; Received in revised form 18 May 2020; Accepted 19 May 2020
Available online 23 May 2020
1053-8119/Crown Copyright © 2020 Published by Elsevier Inc. This is an open access article under the CC BY-NC-ND license (http://creativecommons.org/licenses/by-nc-nd/4.0/).

So far, neuroimaging investigations of the EVC have focused on visual rather than motor imagery, and the results have been controversial, with some studies showing BOLD responses above baseline in the EVC (Chen et al., 1998; Craven and Kanwisher, 2000; Dijkstra et al., 2017; Ganis et al., 2004; Ishai et al., 2002; Klein et al., 2000; Lambert et al., 2002; Le Bihan et al., 1993; Sabbah et al., 1995), while others did not (D'Esposito et al., 1997; Formisano et al., 2002; Knauff et al., 2000; Trojano et al., 2000; Wheeler and Petersen, 2000). Regardless of the involvement of the EVC in perceptual imagery, visual imagery content can be decoded from the EVC even when activation is at baseline (Albers et al., 2013; Dijkstra et al., 2017; Koenig-Robert and Pearson, 2019; Naselaris et al., 2015), and most intriguingly, there are common patterns of activity that are shared between perception and visual imagery (Albers et al., 2013; Naselaris et al., 2015; Pearson et al., 2015).

In addition to the role of the EVC in imagery tasks, it is becoming increasingly recognized that the primary visual cortex (V1) is also involved in high-level cognitive and motor-related functions, including planning and executing object-directed actions, even in absence of online visual information. Pre-movement activity patterns in V1 have been used to successfully decode upcoming actions towards visible targets in fMRI studies (Gallivan et al., 2019; Gutteling et al., 2015). Further, action execution recruits the EVC even when participants perform movements in the dark towards objects that have been visually or haptically explored moments earlier (Monaco et al., 2017; Singhal et al., 2013; Styrkowiec et al., 2019). Could the recruitment of EVC for action be an epiphenomenon of motor imagery? A direct comparison of the activation levels while participants performed or imagined the same actions in the dark, showed that real actions elicit higher activation in the EVC than imagined ones (Monaco et al., 2017). These findings suggest that the visual cortical activation during action execution cannot be entirely explained by motor imagery. In fact, real actions have somatosensory and motor aspects that imagined actions do not have. Specifically, proprioceptive feedback and efference copy resulting from movement execution might affect the activation in the EVC, evoking higher responses for executed than imagined movements. Importantly, unlike action execution, action planning lacks afferent sensory information and outflowing motor signals. Therefore, action planning, rather than action execution, might offer a more balanced comparison for motor imagery. Indeed, it has been proposed that imagined movements are the internal simulation of real movements (Jeannerod and Decety, 1995), and recent behavioural findings suggest that sensorimotor predictions are generated during motor imagery with similar mechanisms as engaged during action planning (Kilteni et al. (2018). Therefore, planning and imagining actions might have similar activity patterns that could indicate a shared representation of their content in the EVC. Yet, the role of V1 in motor imagery has been largely neglected. This understanding is particularly relevant for the development of communication pathways that are independent of muscle activity, an important consideration for the implementation of motor imagery based brain-computer interfaces that aim to decode brain signals into control commands for individuals with severe motor impairments following neuronal disorders that have caused the loss of muscular control (Aflalo et al., 2015; Aggarwal and Chugh, 2019; Batula et al., 2017; Höhne et al., 2014).

Action planning and motor imagery have several aspects in common. First, unlike perception and visual imagery, action planning and motor imagery are both top-down processes that elicit activity across a large neural network spanning frontal to primary sensory areas including the EVC, which receives information through feedback projections from higher-level areas (Markov et al., 2011). Second, both action planning and motor imagery tasks lack a sensory component, which conceptually renders them more similar to each other than perception and visual imagery are. Because motor planning and action imagery do not have incoming sensory or outgoing motor information, the activation level elicited by these tasks is not as high as for other tasks, like motor execution or visual perception. To probe the content of these processes with high sensitivity, we used a pattern classification-based approach, by training a statistical classifier (decoder) to learn a relationship (if any) between fMRI activity patterns and the target contents to be decoded for planned and imagined actions. Successful training should then allow the decoder to predict target contents based on newly presented activity patterns (Haynes, 2015; Norman et al., 2006). Given the limited understanding of the neural mechanisms involved in processing motor imagery in the EVC, and how they relate to action planning, we used multivoxel pattern analysis (MVPA) of fMRI activity to achieve three goals. The first goal was to determine whether imagined actions can be decoded from the activity patterns in the EVC. The second goal was to replicate recent findings showing dissociable patterns of brain activity for different movement plans in the EVC (Gallivan et al., 2019). The third goal, pending success of the first two, was to examine whether action representation can be generalized between imagining and planning actions in the EVC. To achieve these goals, we asked participants to perform delayed tasks in which they either executed one of three movements (i.e., grasp a large or a small object, or reach to touch an object) towards a centrally located target, or imagined performing the same movements after a delay without executing any real action.

We hypothesized that if motor imagery (or action planning) is represented in the EVC, a classifier would show above-chance decoding accuracy of the different imagined (or planned) actions. In addition, if action representation is generalized between planned and imagined movements in the EVC, there would be above chance decoding accuracy of planned actions based on activity patterns elicited by imagined actions, and vice versa. Hence, we used cross-condition classification to examine whether the representation of action is independent of the task giving rise to that representation, i.e., imagining an action or planning a real one (Fig. 1A). Cross-classification is a popular approach in multivariate decoding, and it refers to the ability of a decoder to generalize between different contexts, and asses associations between cognitive processes (Kaplan et al., 2015). As such, if a classifier trained on one context (e.g., motor imagery) can generalize to data from a different context (e.g., action planning), this demonstrate a stable abstract representation of action between both conditions, regardless of whether the action is imagined or planned for real subsequent execution. We have explored these questions not only in the EVC, but also in areas of the parietal and frontal cortex where successful decoding for motor imagery and action planning should be expected. In fact, motor imagery as well as action planning recruit frontal and parietal networks, as examined with univariate and multivariate analyses (Gallivan et al., 2011; Hardwick et al., 2018; Oosterhof et al., 2012; Zabicki et al., 2017). Although the activity patterns in these regions have been found to have a representation of action plans and motor imagery, with the two tasks being investigated in different studies, so far, the direct comparison between motor imagery and action planning has not been examined yet.

2. Methods

2.1. Sessions and subjects

Two fMRI sessions (experiment and retinotopic mapping) and an eye-tracking control experiment took place in three different days. The results of the eccentricity mapping session were used to ensure that the EVC ROI selected with the experimental runs fell within the expected location of the target object. In, fact a recent study has shown accurate decoding of action intention in retinotopic areas of the EVC corresponding to the location of the target object, but not in non-object-related locations (Gallivan et al., 2019). The eye tracking experiment was run to ensure that participants could reliably maintain fixation for the duration of the experiment.

The experimental fMRI session lasted ~2 h, including participant screening and set-up time, while the retinotopic-mapping fMRI session lasted ~20 min. The eye-tracking control experiment lasted ~1 h.

Thirty-five volunteers (age range 20–44, average 30.3, 21 females and 14 males) participated in this experiment. Eighteen participants (age

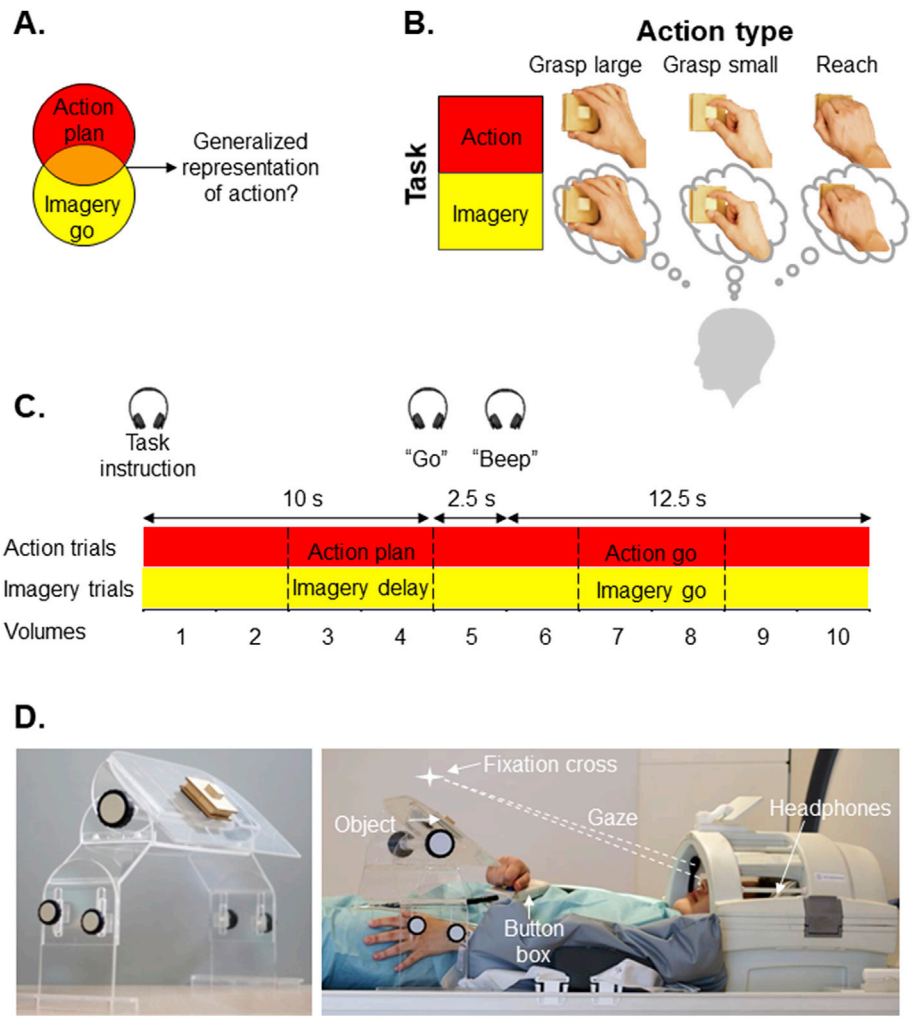

Fig. 1. Image of the experimental question, design, timing and setup. A. Schematic representation of the experimental question: can we decode action types in the EVC based on the activity patterns during action planning (red), action imagery (yellow), and across planning and imagining actions (orange)? **B**. We had a 2 x 3 factorial design with three action types (Grasp large, Grasp small and Reach) and two tasks (Action and Imagery). **C**. At the beginning of each trial, a recorded voice instructed participants about the action they had to perform (in Action trials) or imagine (in imagery trials) at the end of the trial. The recorded voices were: "do grasp large", "do grasp small", "do reach touch", "image grasp large", "image grasp small", "image reach touch". After a delay of 10 s, a "go" cue prompted participants to perform the task. A "beep" sound indicated the end of the trial. We used an inter-trial interval of 12.5 s. We performed MVPA on single trials based on the time phases indicated by the dashed lines. In particular, to examine whether we could decode upcoming actions, we focused the analyses on the pre-movement time-points in Action trials (Action plan), while time-points corresponding to task execution were of critical interest to test whether we could decode imagined actions in imagery trials (Imagery go). **D**. The setup (right panel) required participants to gaze at the fixation point marked with a cross while performing the tasks. The object was placed on a platform (left panel) ~6.5° of visual angles below the fixation point and aligned to the participant body midline.

range 21–43, average 29, 11 females and 7 males) took part in the experimental session and fourteen participants (age range 20–44, average 29.6, 7 females and 7 males) took part in the retinotopic mapping session with fMRI. Four subjects participated in both fMRI sessions. A separate set of seven volunteers (age range 25–41, average 31, 6 females and 1 male) participated in the eye-tracking control experiment. All participants were right-handed and had normal or corrected to normal vision.

This study conforms to the Code of Ethics of the World Medical Association (Declaration of Helsinki)printed in the British Medical Journal (18 July 1964). Ethics approval was obtained from the Human Research Ethics Committee of the University of Trento. Written informed consent was obtained from all participants included in the study.

2.2. Experimental paradigm and design

We used a slow event-related fMRI design to measure the blood-oxygenation-level dependent (BOLD) signal (Ogawa et al., 1992) while participants performed or imagined performing delayed actions towards an object, which consisted of a small block attached on a large block. As shown in Fig. 1B, the actions consisted of grasping the large block (Grasp large), grasping the small block (Grasp small), and reaching to touch the object (Reach). Participants performed the actions using their right (dominant) hand. The object was viewed directly by the participants without mirrors (Culham et al., 2003).

We used an experimental paradigm similar to the one recently described in (Monaco et al., 2019). Each trial started with an auditory task instruction that informed the participant about the task (Action or Imagery) and the action type (Grasp large, Grasp small, Reach) to be performed or imagined at the end of the trial. The onset of the task instruction was followed by the onset of a "go" cue 10 s later that prompted participants to perform or imagine the action. A "beep" sound after 2.5 s signaled the end of the trial and cued participants to return or imagine returning the hand to the home position in action and imagery trials, respectively. The purpose of the "beep" sound was twofold. First, it ensured that real and imagined actions had similar durations. Second, it allowed us to keep as constant as possible the duration of the return phase of different movements types (grasp large, grasp small, and reach), avoiding that potential differences in brain activity patterns between action types in the Action go phase could be related to different durations of the inward movement to return the hand to the home position. The next trial started after 12.5 s of inter-trial interval (ITI) (Fig. 1C). This duration of the intertrial interval enabled the fMRI response to go back to baseline level before the next trial started, avoiding contaminations of the BOLD signal in the subsequent trial (Gallivan et al., 2011; Monaco et al., 2019, 2011; Singhal et al., 2013). The target object was presented for the full duration of the trial; therefore the visual information about the object was constant within and between trials. Participants grasped the large object with a whole-hand grasp and the small object with a precision grip. During reach actions participants reached the object and touched it with the knuckles. Participants were asked to fixate a cross placed above the object, therefore the object was in the participant's lower visual field, at ~6.5°of visual angles. This set-up allowed participants to maintain their gaze at a comfortable location on the fixation

point without straining the eyes, while viewing the object in the lower visual field. This is an important consideration aimed to avoid having participants move their eyes during the experiment. In addition, this configuration resembles many everyday life situations in which we reach out to grasp objects in our lower peripheral visual field, like when we reach out to grasp a computer mouse while fixating the monitor or the gear stick while driving a car.

At the end of each trial, participants returned the hand to a button box placed at a comfortable location around the navel. Participants kept the button pressed during the intertrial interval by resting their hand on it until they started the next movement. This enabled us to acquire reaction times (RT) and movement times (MT) during Action trials.

The two tasks (Action and Imagery) and three action types (Grasp large, Grasp small and Reach) gave rise to a two by three factorial design with six conditions: Action Grasp large, Action Grasp small, Action Reach, Imagery Grasp large, Imagery Grasp small, Imagery Reach (Fig. 1B).

A video camera placed in the magnet room recorded the actions performed by the participants for off-line investigation of the errors. Errors could take the form of mistakes in the performance of the task (e.g., initiating a movement before the "go" cue or performing an action in an imagery trial) and were excluded from further analyses. In total, 2.1% of trials were discarded from the analyses because of such errors.

Each run lasted approximately 13 min and included 5 trials per experimental condition, for a total of 30 trials per run. The six trial types were pseudorandomized within each run and presented in counterbalanced order across all runs so that each trial type was preceded and followed equally often by other trial types across the experiment. Participants completed five functional runs for a total of 150 trials per subject (25 trials per condition).

2.2.1. Apparatus

Goal-directed actions were performed towards a wooden object located on a platform which was secured to the bore bed (Fig. 1D, left panel). The platform was made of Plexiglas and its location could be adjusted to ensure that the participant could comfortably reach the stimulus. The head of the participant was tilted by ~20° to allow direct viewing of the stimuli. The height of the platform could also be adjusted to improve the view and the reachability of the object for each participant. The right upper arm of the participant was supported with foam, and the left arm rested beside the body (Fig. 1D, right panel).

The target object (small block: 2.5 by 2.5 cm, large block: 7 × 7 cm) was affixed to the platform with Velcro. The surface of the platform where the object was attached was covered with the complementary side of the Velcro. The platform was placed approximately 10 cm above the subject's pelvis at a comfortable and natural grasping distance. The stimulus was positioned in the same central location throughout the experiment. The fixation cross was placed ~6.5 cm above the object at a viewing distance of ~57 cm, such that 1 cm in the visual field corresponded to ~1 degree of visual angle. Auditory cues were played through Presentation software, which was triggered by a computer that received a signal from the MRI scanner.

2.3. Imaging parameters

This study was conducted at the Center for Mind/Brain Sciences (University of Trento, Italy) using a 4-Tesla Bruker MedSpec Biospin MR scanner and an 8-channel head coil. Functional data were acquired using T2*-weighted segmented gradient echo-planar imaging sequence (repetition time [TR] = 2500 ms for experimental runs, 2000 ms for eccentricity mapping; echo time [TE] = 33 ms; flip angle [FA] = 78° for experimental runs, 73° for eccentricity mapping; field of view [FOV] = 192 × 192 mm, matrix size = 64 × 64 leading to an in-slice resolution of 3 × 3 mm; slice thickness = 3 mm, 0.45 mm gap). Each volume comprised 35 slices acquired in ascending interleaved order. At the beginning of each experimental session, a T1-weighted anatomical reference volume was acquired using a MPRAGE sequence (TR = 2700 ms; inversion time TI = 1,020 ms; FA = 7°; FOV = 256 x 224, 176 slices, 1 mm isotropic resolution).

2.4. Preprocessing steps and general linear model (GLM)

We analyzed the imaging data using the BrainVoyager QX software (Brain Innovation 2.8, Maastricht, The Netherlands). Functional data were superimposed on anatomical brain images, aligned with the anterior commissure–posterior commissure line, and transformed into Talairach space (Talairach and Tournoux, 1988). The first four volumes of each fMRI scan were discarded to allow for T1 equilibration. Functional data were preprocessed with temporal smoothing to remove frequencies below 2 cycles per run. Slice-time correction with a cubic spline interpolation algorithm was also performed. Functional data from each run were screened to ensure that no obvious motion artifacts (e.g., rims of activation) were present in the activation maps from individual participants.

Each functional run was motion corrected using a trilinear/sinc interpolation algorithm, such that each volume was aligned to the volume of the functional scan closest to the anatomical scan. The motion correction parameters of each run were also checked. Data from two participants showed abrupt head motion over 1 mm between successive volumes and were discarded from further analyses.

We used a group random effects (RFX) GLM to run a deconvolution analysis (Glover, 1999) rather than using the convolution approach with a standard hemodynamic response function (HRF). Specifically, we estimated the amplitude of the BOLD signal at each time point for each condition by using an impulse response function, also known as stick function. The deconvolution analysis allowed us to isolate and have an accurate estimate of the brain activity during the planning phase preceding action execution without risking contamination of the brain signal from the subsequent movement phase due to imperfect predictor functions convolved with the assumed HRF (for a similar procedure see Ariani et al., 2015).

We had six conditions (2 Tasks x 3 Action types) and ten time points (spike predictors) for each trial resulting in 60 predictors of interest. We also included movement parameters (3 rotations and 3 translations), and error trials as predictors of no interest.

2.5. Eccentricity mapping

The expanding ring, used for eccentricity mapping, increased logarithmically as a function of time in both size and rate of expansion, so as to match the estimated human cortical magnification function (for details, see Swisher et al., 2007). The smallest and largest ring size corresponded, respectively, to 1° and 10° of diameter. We divided the 10° into 8 equal time bins (of 8 s each). The eccentricity mapping localizer was composed of 8 cycles, each lasting 64 s. A fixation time was added at the beginning and at the end of the experiment for a total duration of 9 min per run. The stimuli were rear-projected with an LCD projector (EPSON EMP 7900 projector; resolution, 1280x1024, 60-Hz refresh rate) onto a screen mounted behind the participants head. The participants viewed the images through a mirror mounted to the head coil directly above the eyes, and were asked to fixate a dot at the center of the screen without performing any task. For eccentricity stimuli, we convolved a boxcar-shaped predictor for each bin with a standard HRF and performed contrasts using an RFX GLM.

We used the results of the eccentricity mapping session to ensure that the ROI selected with the experimental runs in the EVC fell within the expected location of the target object, corresponding to eccentricities above 6.5° of visual angles.

2.6. Statistical analysis

We explored the role of action panning and motor imagery in ten regions of interest (ROIs) in the left and right hemisphere, spanning from

areas known to be specialized in visual processing, (i.e., early visual cortex), to areas specialized in motor functions (i.e. primary motor and somatosensory cortex), as well as parietal and frontal regions known to be involved in action planning and motor imagery (i.e., dorsal and ventral premotor cortex and anterior intraparietal sulcus) (Gallivan et al., 2011; Hardwick et al., 2018).

Our questions were aimed to determine whether:1) planned and imagined actions can be decoded from fMRI activity patterns, and 2) action content can be generalized across planning and imagining movements. To this aim, we chose to compare action imagery to action planning, rather than action execution, in order to avoid contamination of the brain activity by somatosensory, proprioceptive, visual and motor responses that are present when performing an action, but not while imagining or planning a movement. As such, we focused our analyses on the planning phase preceding action execution in Action trials, and the execution phase of Imagery trials. Specifically, in our key comparisons,

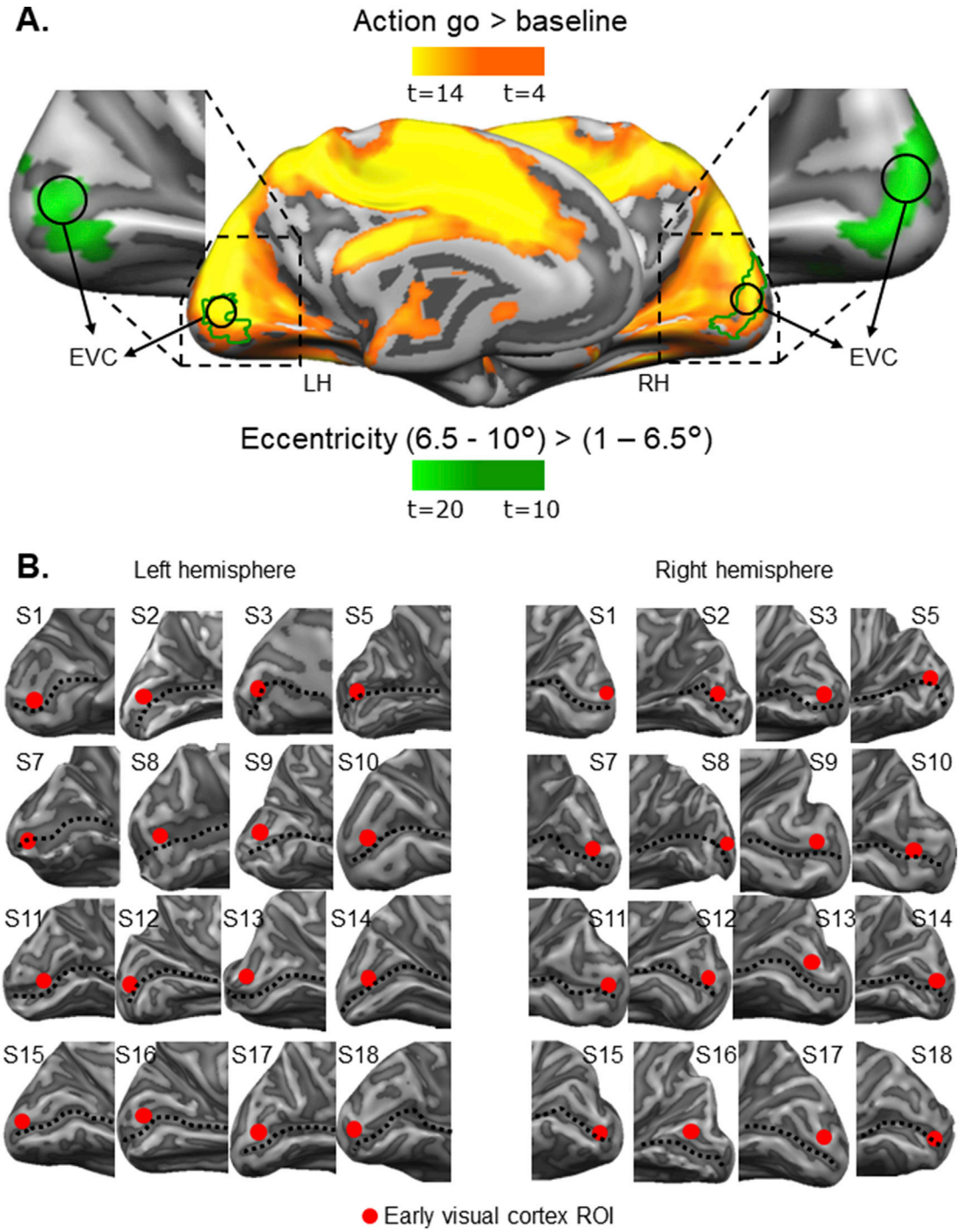

Fig. 2. Voxelwise activation and groupearly visual cortex ROIs(A), and early visual cortex ROIs in individual participants (B). A. Voxelwise statistical maps obtained with group random effects (RFX) GLM of the experimental runs (yellow-orange map) and eccentricity mapping (light-dark green map). Activation maps are overlaid on the average cortical surface derived from the cortex-based alignment performed on 16 participants. The group EVC ROI was defined in left and right hemisphere as a sphere in the area of overlap between the map showing higher activation during action execution in the experimental runs (yellow) and the region corresponding to eccentricities higher than 6.5° of visual angles (green) on or slightly above the calcarine sulcus, consistent with the location of the object below the fixation point. **B**. Spheres (6-mm radius) for individual EVC ROIs in each participant for left and right hemisphere.

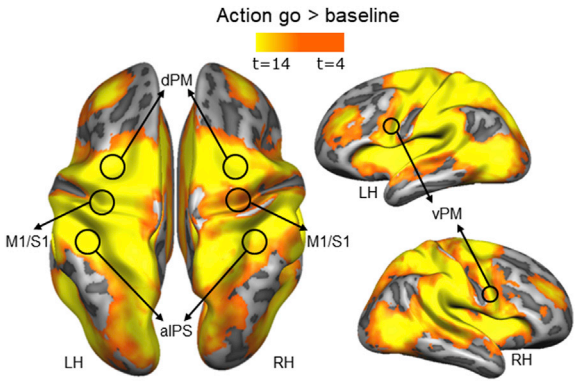

Fig. 3. Voxelwise activation in the action network. Group ROIs in the action network showing higher activation for action execution vs baseline.

for the plan phase time points in Action trials, we extracted the mean of volumes 3–4 (Action plan), which correspond to the two volumes immediately before participants executed the task. For the go phase time points in Imagery trials, we extracted the mean of volumes 7–8 (Imagery go), which correspond to the peak of the transient real or imagined action (Fig. 1C). In addition, we performed control analyses on the mean of volumes 3–4 of Imagery trials (Imagery delay) and volumes 7–8 of Action trials (Action go).

We identified the zone of the early visual cortex (EVC) corresponding to the retinotopic location of the object in the lower visual field, as well as control ROIs in the action network known to be involved in movement execution and motor imagery. To this aim, we contrasted activity for action execution against baseline: [Action go (grasp large, grasp small, reach) > baseline]. This univariate contrast allows identification of the portion of the early visual cortex (EVC) above the calcarine sulcus corresponding to the location of the object in the lower visual field, as well as areas involved in action in the dorsal visual stream. Contrasts were performed on %-transformed beta weights (β), therefore β values are scaled with respect to the mean signal level. The selection criteria were independent from the key comparison explored in further analyses and prevented any bias towards our predictions (Kriegeskorte et al., 2010; Vul et al., 2010).

We localized individual ROIs with the following steps. First, we outlined the areas based on the group activation map obtained with the RFX-GLM contrast: (Action go > baseline), by circumscribing group ROIs (6-mm radius) around their expected anatomical landmarks (Figs. 2A and 3). Second, within each group ROI we defined individual ROIs, separately for each participant, as spheres with radius of 6 mm centered around each individual peak voxel resulting from the single-subject GLM contrasts (Action go > baseline) (see Fig. 2B for individual EVC ROIs). This approach ensured that all regions were objectively selected, and that all ROIs had the same number of anatomical voxels (925 mm^3). The averaged Talairach coordinates of individual ROIs are shown in Table 1.

To ensure that the group ROIs in the EVC fell within the retinotopic location of the object in the calcarine sulcus, we used the results of the eccentricity mapping at the group level. We reasoned that since the object was located ~6.5 cm below the fixation point at a viewing distance of ~57 cm (where 1 cm corresponded to 1 degree of visual angle), we could localize its location in the visual cortex at eccentricities higher than 6.5° of visual angle on or slightly above the calcarine sulcus, consistent with the location of the object in the lower visual field (Fig. 2A, green activation maps in lateral panels). We then identified the overlap between the activation map for eccentricities corresponding to 6.5–10° of visual angle, and the activation map obtained with the univariate contrast (Action go > baseline), as the object was visible during the execution phase (Fig. 2A, yellow activation map in central panel). The sphere corresponding to the group EVC ROI was drawn within the overlapping region in both hemispheres. Individual ROIs were defined by selecting the voxel around the peak functional activation for the univariate contrast (Action go > baseline) within the group EVC ROIs for each participant (Fig. 2B).

Table 1
Talairach coordinates averaged across all participants for each ROI. Note: LH: left hemisphere; RH: right hemisphere. All ROIs have the same number of anatomical voxels (925 mm^3).

	Talairach Coordinates		
	X	Y	Z
LH EVC	−10	−87	3
RH EVC	7	−85	5
LH dPM	−28	−17	50
RH dPM	20	−13	49
LH vPM	−46	5	23
RH vPM	41	0	19
LH M1/S1	−35	−30	45
RH M1/S1	31	−28	45
LH aIPS	−43	−31	37
RH aIPS	41	−33	37

We identified eight ROIs in the dorsal visual stream known to be involved in action planning and execution (Gallivan et al., 2011), as well as motor imagery (Hardwick et al., 2018) based on the univariate RFX-GLM contrast (Action go > baseline). In particular, we identified bilateral dorsal and ventral premotor areas (dPM and vPM), primary motor/somatosensory area (M1/S1) and anterior intraparietal sulcus (aIPS). As shown in Fig. 3, at the group level the dorsal premotor cortex (dPM) was identified at the junction of the superior frontal sulcus and the precentral sulcus (Monaco et al., 2014). The primary motor and somatosensory cortex (M1/S1) was localized by selecting voxels encompassing the pre- and post-central gyri in correspondence of the omega-shaped hand knob. The ventral premotor cortex (vPM) was identified by selecting voxels slightly inferior and posterior to the junction of the inferior frontal sulcus and precentral sulcus (Gallivan et al., 2011). The anterior intraparietal sulcus (aIPS) was localized at the junction of the intraparietal sulcus and the inferior segment of the postcentral sulcus (Culham et al., 2003). Individual ROIs were defined by selecting the voxel around the peak functional activation for the univariate contrast (Action go > baseline) within the group ROI for each participant.

2.6.1. Univariate analysis

Our first question was aimed to determine whether brain activity can be used to determine the content of motor imagery, as well as action plans. Therefore, we initially investigated the overall activation levels within each ROI for the key comparisons between action types. To do so, for each ROI from each participant we extracted the activation magnitude (β weights) from the Action plan and Imagery go phase and used it for further analyses. For each area, we performed an ANOVA on the activation magnitude (β weights) with 2 tasks (Action plan, Imagery go) and 3 action types (Grasp large, Grasp small, Reach). To further illustrate whether activation levels were above baseline for Action plan and Imagery go tasks, we performed two-tailed one-sample t-tests against baseline and computed 95% confidence limits.

2.6.2. Multivoxel pattern analysis (MVPA)

MVPA was performed with the CoSMo MVPA Toolbox for MATLAB (publicly available at http://www.cosmomvpa.org, Oosterhof et al., 2016), adopting a Linear Discriminant Analysis (LDA) classifier (http://cosmomvpa.org/matlab/cosmo_classify_lda.html#cosmo-classify-lda). For each participant and for each of the 10 ROIs, we estimated β weights on non-spatially-smoothed data using the design matrix outlined in the GLM. We decoded activity patterns from individual runs and used a 'leave-one-run-out' cross-validation approach to estimate the accuracy of the LDA classifier.

To answer our first question about whether motor imagery content, as

well as action plans, can be decoded from activity patterns in our ROIs, multiple binary classifiers were trained to discriminate between two movement types within each of the three pairs of movements (Grasp large vs. Grasp small, Grasp large vs. reach, and Grasp small vs. Reach) separately for the Action plan (volumes 3–4) and Imagery go phase (volumes 7–8) of Action and Imagery trials, respectively. Classification accuracies were then combined to produce an average accuracy for each ROI. To answer our second question about whether action representations generalize between planning real actions and imagining them, we performed cross-condition decoding. Specifically, we trained the classifier on the dissociation between movement pairs in one phase of one task (e.g., Grasp large vs Grasp small during the Action plan in Action trials) and tested the performance of the classifier to distinguish between the same pair of movements in another phase of the other task (e.g., Grasp large vs Grasp small during Imagery go in Imagery trials), and vice versa. Again, the average of the three binary classifiers was computed to produce one accuracy value for each ROI. Results from the two cross-condition decoding analyses (i.e., train on Action plan, test on Imagery go and vice versa) were also averaged.

We assessed statistical significance of the classification accuracies (averaged across the three binary classifiers) with a two-tailed one-sample *t*-test across participants against chance decoding (50%) for each ROI. Statistical results were corrected for multiple comparisons (number of ROIs x number of tests) using the False Discovery Rate method (FDR) (Benjamini and Yekutieli, 2001).

To examine classification performance in regions that are not expected to show predictive power, we additionally included three control ROIs where we expected no statistically significant classification. In particular, the control ROIs were spheres with radius of 6 mm, and were located within each participant's left: 1) ventricle, 2) white matter, and 3) grey matter. The control cortical ROI in the grey matter was chosen in order to have an optimal term of comparison for the other cortical ROIs of interest, in terms of the characteristics of brain tissues. We selected the ROI in the grey matter of the orbital gyrus, known to be implicated in sensory and cognitive functions (i.e., perception of odors and emotion regulation, Bechara, 2004; Shepherd, 2007) that are substantially different from the ones investigated in the current study.

2.6.3. Behavioural analysis

Reaction and movement times were measured in Action trials during the fMRI experiment. The RTs were calculated as the time elapsed from the "go" cue to button release, while the MTs consisted of the duration of a movement measured from button release to button press. As such, MTs included not only the outward movement, as MTs are typically measured, but also the inward one. In an effort to isolate the variability of outward movements, we kept the duration of the inward phase as constant as possible by introducing a "beep" sound, which cued participants to return the hand to the home position after each movement (Fig. 1C). To evaluate differences between conditions, we ran a one-way ANOVA with repeated measures for each dependent variable (RT and MT). Behavioural data from two participants out of 16 could not be recorded for technical reasons. It is worth noting that behavioural differences between conditions during the go phase in Action trials might be reflected in differences in brain signals during the corresponding time points.

2.7. Subjective vividness rating

The ability to create vivid motor images varies not only between individuals, but also within a lifespan (Isaac and Marks, 1994). In addition, there is a relation between motor ability and neural activity, with stronger activations in parietal and frontal cortex in individuals with good imagery ability (Guillot et al., 2008), and correlations in V1 between neural activity and kinesthetic motor imagery (Mizuguchi et al., 2016). Given the relationship between motor imagery and neural activity, and since we used an fMRI task based on motor imagery, we assessed the motor imagery vividness in our participants to ensure that they showed generally good imagery ability. As such, at the end of the experimental session, eight participants completed a Vividness of Motor Imagery Questionnaire (VMIQ-2) designed to measure the quality of their visual and kinesthetic imagery of motor tasks (Roberts et al., 2008). The questionnaire assesses whether participants have a robust mental experience, and requires individuals to imagine themselves performing 12 activities from three imagery perspectives: external visual imagery (EVI; a third-person perspective), internal visual imagery (IVI; a first-person perspective), and kinesthetic imagery (KI; feeling the movement). Each action is rated by each individual on a scale from 1 (vivid imagery) to 5 (no imagery).

We calculated the average vividness rating for each imagery perspective as an indication of the participants' imagery ability. Then, we calculated a Pearson's correlation coefficient (r) to examine whether there was a relationship between vividness scores and classifier accuracies in our ROIs, as well as between vividness scores and % signal change. In particular, for each individual, we extracted the β weights from each ROI, averaged them across the three imagery conditions (Imagery grasp large, Imagery grasp small and Imagery Reach), and correlated them with the subjective vividness scores for each of the three imagery perspectives.

2.8. Eye-tracking control experiment

To validate whether individuals can reliably maintain fixation over the course of the experiment, we replicated the same experiment outside the MRI scanner while participants' eye movements were monitored using an EyeLink 1000 Plus eye tracker (SR Research). A separate set of seven participants completed the full experiment while monocular eye-tracking was performed at a sample rate of 1000 Hz. Participants sat in front of a table with the head resting on a chinrest and performed or imagined actions towards the object placed on the platform above the table. As in the fMRI experiment, the object was located ~6.5 cm below a fixation cross displayed on a monitor at a viewing distance of ~57 cm. Participants rested the right hand at a comfortable position on the table in front of them, and performed the action when prompted by the "go" cue in Action trials. No real action was performed in imagery trials. We could not monitor eye movements during the fMRI session as there are no MR-compatible eye trackers that can monitor gaze in the head-tilted configuration, because of occlusion from the eyelids. Unlike the fMRI experiment, during the eye-tracking control experiment participants were sitting upright. Despite this difference, the control experiment could give us an indication about whether, in general, participants are able to reliably maintain fixation over the course of the full experiment. If so, accurate decoding performance in frontal, parietal and visual cortices is unlikely to be due to eye movements or differences in retinal inputs in different tasks.

We determined the accuracy and precision of participants' eye positions by computing the constant error (overall bias in the average location of fixation relative to the central cross) and standard deviation in horizontal and vertical dimensions for each condition and phase of the trial that was used for fMRI analyses.

3. Results

3.1. Motor imagery ability

Overall, participants' scores in the VMIQ-2 indicated average imagery ability (EVI average VMIQ-2 score: 2.5, range 1.5–3.6; IVI average VMIQ-2 score: 2.2, range 1.3–2.8; KI average VMIQ-2 score: 2.3, range 1.2–3.2). Paired sample t-tests did not reveal any significant differences between the three types of motor imagery perspectives. The average VMIQ-2 scores for each participant across the three imagery perspectives ranged from 1.4 (close to "Perfectly clear and as vivid as normal vision or feel of movement") to 2.9 (close to "Moderately clear and vivid"), and the overall average VMIQ-2 score was 2.3 (close to "Clear and reasonably

Table 2
Average reaction and movement times with corresponding standard deviations.

	Grasp large	Grasp small	Reach
RTs (ms)	943 ± 178	937 ± 164	386 ± 8
MTs (ms)	3179 ± 431	3104 ± 460	2982 ± 446

Note: In Action trials, RTs and MTs are longer for grasp than reach movements.

vivid"). The analysis of internal consistency of the VMIQ-2 revealed a Cronbach's alpha of 0.96, 0.82 and 0.9 for EVI, IVI and KI, respectively, indicating relatively high internal consistency. There was no significant correlation between % signal change and vividness scores (p at most = 0.471), or between classifier accuracies and vividness scores (p at most = 0.059) in any of our ROIs. All participants reported using imagery from the first-person perspective during the fMRI experiment.

3.2. Behavioural results

As shown in Table 2, participants were faster to initiate and complete reach than grasp movements, regardless of whether they were required to grasp the large or small object. In particular, we found a main effect of Action Type in RTs ($F_{(1, 14)} = 140.6$, $p < .00001$) and MTs ($F_{(1, 14)} = 8.2$, $p = .002$). Paired sample t-tests indicated longer RTs and MTs for Grasp large than Reach (RT: $t = 11.6$, $p < .00001$; MT: $t = 3.3$, $p = .02$) and Grasp small than Reach (RT: $t = 12.6$, $p < .00001$; MT: $t = 3.1$, $p = .03$), but not for Grasp large vs. Grasp small (RT: t=.47, $p = 1$; MT: $t = 1.6$, $p = .37$).

3.3. Eye-tracking results

The results of the control eye-tracking experiment showed that participants' fixation was accurate and precise. Specifically, the constant error during Action plan and Imagery go phases was negligible, with averages at −0.07° and −0.15° degrees for the horizontal axis, and −0.14° and 0.15° degrees for the vertical axis. Further, the standard deviation during Action plan and Imagery go phases was on average at 0.4° for the horizontal axis, and 0.37° and 0.55° for the vertical axis. Importantly, the 2 x 3 ANOVAs (i.e. 2 tasks × 3 action types) revealed no statistically significant main effect or interaction for either constant error or standard deviation in horizontal and vertical dimensions ($p > 0.05$ for all comparisons). These results demonstrate that generally individuals can reliably maintain fixation during the full experiment and, as such, eye movements are unlikely to account for accurate decoding performance in visual as well as frontal and parietal cortices.

3.4. fMRI results

3.4.1. Univariate analysis

The univariate analyses showed a main effect of Task with higher activation for Imagery go than Action plan in bilateral aIPS and vPM (Fig. 4, Table 3). However, there was no main effect of movement type and no interaction in any of the ten ROIs. The average activation level for Action plan was higher than baseline in right EVC, left dPM and vPM, while Imagery go elicited above baseline activation in all areas except for the EVC.

3.4.2. Multivoxel pattern analysis

We used MVPA in each ROI to test whether action types could be decoded on the basis of patterns of brain activity during action planning, action imagery and across action planning and imagery. Tables 4 and 5 show the statistical values for all ROIs.

Fig. 2B shows the EVC in the left and right hemisphere of each participant. Decoding accuracies averaged across participants are shown in Fig. 5. In bilateral EVC, we found significant decoding of movement type during action planning and imagery (red and yellow plots), but not across Action plan and Imagery go (orange plots, see Table 4 for

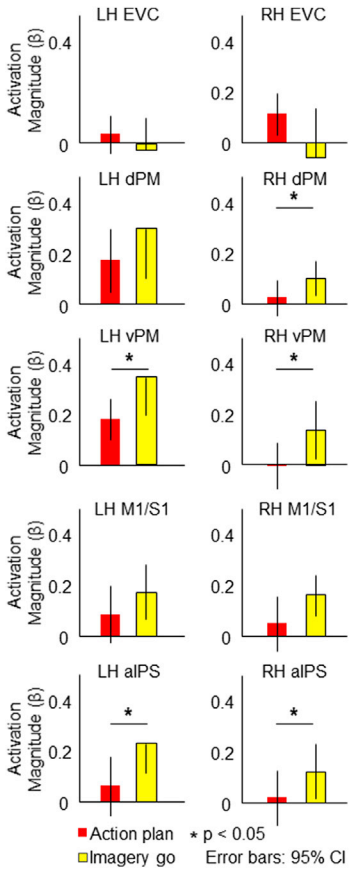

Fig. 4. Univariate results shown as activation levels in our ROIs. For each area, the bar graphs indicate the β weights for the main effect of Task (Action and Imagery) extracted from the Action plan phase of Action trials (red bars) and the Imagery go phase of Imagery trials (yellow bars) from individual ROIs of each participant. Error bars show 95% confidence intervals. Note that activation levels during action planning are at baseline for most areas. In addition, while the EVC shows activation at baseline also for motor imagery task, pattern-based classification analyses show representation of planned as well as imagined actions in several areas spanning the visual, parietal and frontal cortex (Figs. 5 and 6).

Table 3
Statistical values for univariate analysis results.

	Main effect of task, $F_{1,15}$ Imagery go > Action plan	Action plan > baseline, t(15)	Imagery go > baseline, t(15)
LH EVC	p=.24 F=1.49	p=.39 t=.89	p=.66 t=.45
RH EVC	p=.14 F=2.38	**p=.017 t=2.68**	p=.643 t=0.47
LH dPM	p=.12 F=2.71	**p=.01 t=2.76**	**p=.009 t=3**
RH dPM	**p=.017 F=7.17**	p=.51 F=.68	**p=.01 t=2.93**
LH vPM	**p=.019 F=6.9**	**p=.0004 t=4.53**	**p=.0004 t=4.56**
RH vPM	**p=.05 F=4.56**	p=.93 t=.9	**p=.03 t=2.34**
LH M1/S1	p=.14 F=2.46	p=.16 t=.48	**p=.006 t=3.16**
RH M1/S1	p=.1 F=3.06	p=.37 t=.92	**p=.001 t=3.95**
LH aIPS	**p=.005 F=10.85**	p=.28 t=1.11	**p=.001 t=3.9**
RH aIPS	**p=.03 F=5.51**	p=.73 t=.34	**p=.04 t=2.23**

Note: Statistically significant values are indicated in boldface. Activation level for action planning is at baseline in most areas. Motor imagery does not elicit above baseline activation in the EVC.

Table 4
Statistical values for MVPA results of key comparisons.

	Decoding accuracy for action type, t(15)		
	Action plan	Imagery go	Cross-condition
LH EVC	**p=.004 t=3.32**	**p=.015 t=2.73**	p=.49 t=.71
RH EVC	**p=.022 t=2.55**	**p=.02 t=2.68**	p=.64 t=0.47
LH dPM	**p=.000001 t=5.28**	**p=.002 t=3.66**	**p=.03 t=2.37**
RH dPM	**p=.00003 t=4.61**	**p=.04 t=2.3**	p=.05 t=2.1
LH vPM	**p=.003 t=3.47**	p=.1 t=1.76	p=.08 t=.22
RH vPM	**p=.003 t=3.47**	p=.09 t=.1	**p=.03 t=2.34**
LH M1/S1	**p=.001 t=4.09**	p=.06 t=2.04	p=.57 t=0.58
RH M1/S1	**p=.03 t=2.4**	p=.24 t=1.21	p=.85 t=.19
LH aIPS	**p=.005 t=3.3**	**p=.00005 t=5.01**	**p=.02 t=.25**
RH aIPS	**p=.006 t=3.16**	**p=.03 t=2.33**	**p=.0002 t=4.92**

Note: Statistically significant values are indicated in boldface. Decoding accuracies for the discrimination between different action types are significantly above chance level in the EVC and areas of the action network for action planning. While the activity patterns in most areas allow above chance decoding for motor imagery, only the anterior parietal and premotor cortices show above chance cross-condition decoding.

Table 5
Statistical values for MVPA results of control comparisons.

	Decoding accuracy for action type, t(15)		
	Action go	Cross-phase	Imagery delay
LH EVC	**p=.0001 t=5.1**	**p=.01 t=2.96**	p=.8 t=.3
RH EVC	**p=.036 t=2.3**	p=.29 t=1.09	p=.93 t=.92
LH dPM	**p=.01 t=2.75**	**p=.03 t=2.35**	p=.3 t=1.07
RH dPM	**p=.02 t=2.43**	p=.21 t=1.31	p=.133 t=1.59
LH vPM	**p=.0001 t=4.81**	p=.13 t=1.58	p=.052 t=2.11
RH vPM	**p=.001 t=3.95**	p=.66 t=.44	p=.36 t=.95
LH M1/S1	**p=.0001 t=5.02**	p=.19 t=1.58	p=.91 t=.12
RH M1/S1	**p=.02 t=2.67**	p=.19 t=1.37	p=.94 t=.07
LH aIPS	**p=.0005 t=4.44**	**p=.04 t=2.28**	p=.33 t=1.01
RH aIPS	**p=.03 t=2.39**	p=.23 t=1.25	p=.91 t=.11

Note: Statistically significant values are indicated in boldface. As expected, the activity pattern in all areas allows discriminating between different action types during the execution phase (Action go). Cross-phase decoding accuracy on the plan and go phase of Action trials is above baseline in the early visual, anterior parietal and premotor cortex. No decoding is possible during the delay phase of imagery trials (Imagery delay).

statistical values of all comparisons), suggesting that the representation of actions does not generalize between planning real actions and imagining them in areas specialized in processing low level visual features of objects.

The voxel patterns within several areas of the dorsal visual stream enabled the accurate decoding of the dissociation between movement types during action planning as well as imagery (Fig. 6). As expected, pattern classification in bilateral dPM, vPM, aIPS and left M1/S1 showed successful decoding of movement plans. However, the decoding of movement types for imagery was constrained to left dPM and aIPS. These results show that the activity patterns in left dPM and aIPS flexibly represent movement types regardless of whether the action is planned or imagined. Interestingly, bilateral aIPS shows accurate decoding across Action plan and Imagery go, suggesting that movement types are coded using similar neural mechanisms. Cross-condition decoding was marginal in dPM (see Table 4 for statistical values of all comparisons).

In addition to the key comparisons aimed to answer our questions, we ran an additional set of control comparisons to assess three potential arguments. First, since in Action trials, participants could see their hand during the movements after the "go" cue, we reasoned that visual as well as somatosensory and motor information should allow for statistically significant decoding accuracy for actions in EVC as well as areas in the dorsal visual stream. To examine this, we tested the performance of the classifier to distinguish between action types during movement execution (Action go, volumes 7–8 of in Action trials). Indeed, decoding accuracy

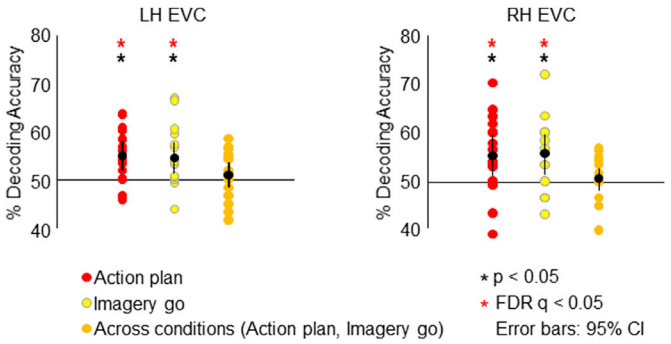

Fig. 5. Classifier decoding accuracies for the discrimination between different action types in early visual cortex ROIs. The scatterplots show decoding accuracies for each participant along with the average (black circles) in left and right hemisphere EVC for the dissociation between the three movement types (grasp large, grasp small, reach) during the planning phase of Action trials (red circles), the go phase of Imagery trials (yellow circles) and across Action plan and Imagery go (orange circles). Chance level is indicated with a line at 50% of decoding accuracy. Error bars show 95% confidence intervals. Black asterisks indicate statistical significance with two-tailed t-tests across subjects with respect to 50%. Red asterisks indicate statistical significance based on an FDR correction of $q < 0.05$. The classifier can accurately discriminate different action types based on activity patterns elicited during action planning (red circles) and motor imagery (yellow circles). However, cross-condition classification (orange circles) is not significant, suggesting that action representation can not be generalized between planning and imagining actions in the EVC.

was significantly above chance in all areas (green plots in Fig. 7, and first column of Table 5 for statistical values). Second, the lack of cross-decoding between Action plan and Imagery go in most of our ROIs, including the EVC (orange plots in Fig. 6), might be related to the fact that the cross-condition decoding is based on different phases of a trial (i.e., before the "go" cue in Action trials and after the "go" cue in Imagery trials), and this might reduce the likelihood of accurate decoding. Should this be the case, cross-decoding accuracy would be at chance level also within the same trial type (cross-phase decoding within Action trials). To assess whether this was the case, we tested the ability of the classifier to dissociate between action types across the two phases of Action trials. Specifically, we trained the classifier to distinguish between movement pairs in the Action plan phase, and tested it in the Action go phase. The results of this test show significantly above chance decoding accuracy in left EVC, dPM and aIPS (light-blue plots in Fig. 7, p uncorrected for dPM and aIPS; statistical values are reported in the second column of Table 5), suggesting that it is unlikely that the lack of decoding accuracy across Action plan and Imagery go, especially in the EVC, is due only to the impossibility to decode across different trial phases. Third, since participants were instructed to imagine movements only after the "go" cue in imagery trials, it should not be possible for the classifier to distinguish between action types during the delay preceding the "go" cue in Imagery trials (Imagery delay, volumes 3–4 of imagery trials). However, not all mental imagery is voluntary (Pearson and Westbrook, 2015); as such, the auditory cue at the beginning of the trial might have triggered the mental image of the action despite participants were instructed to perform the mental task only after the "go" cue. This control analysis did not reveal evidence of dissociable representations during the imagery delay in any of our ROIs (Fig. 7, fuchsia plots, and third column of Table 5 for statistical values). Therefore, while involuntary motor imagery might have taken place immediately after the auditory instruction, this mental process could not be detected in our ROIs.

As a control for our decoding accuracies, we ran the same classification analyses in three control ROIs in the left ventricle, white matter and grey matter in orbital gyrus, where no significant decoding accuracy should be possible. In fact, the results show no dissociable representation for any condition (Fig. 8).

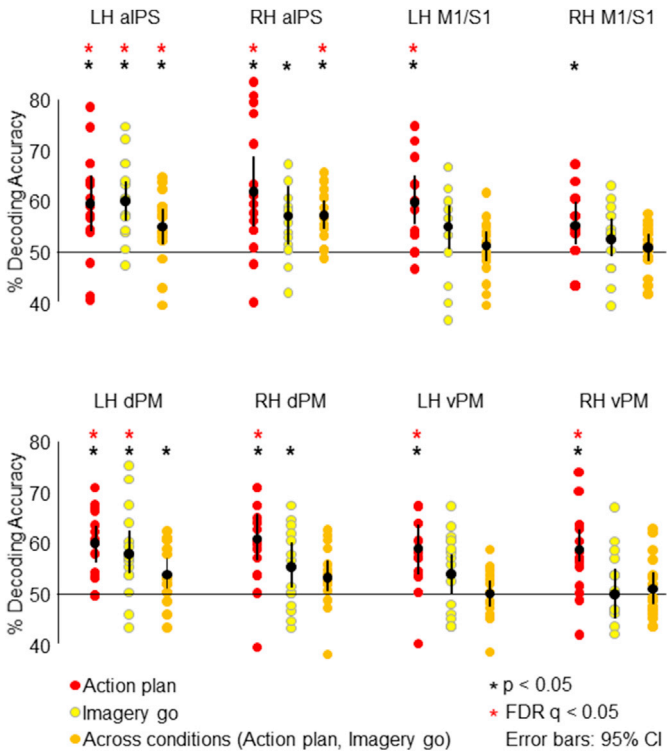

Fig. 6. Classifier decoding accuracies in frontal and parietal ROIs. The scatterplots show decoding accuracies for each participant along with the average (black circles) in frontal and parietal areas in left and right hemisphere for the dissociation between the three movement types during the planning phase of Action trials (red circles), the go phase of Imagery trials (yellow circles) and across Action plan and Imagery go (orange circles). Chance level is indicated with a line at 50% of decoding accuracy. Error bars show 95% confidence intervals. Black asterisks indicate statistical significance with two-tailed t-tests across subjects with respect to 50%. Red asterisks indicate statistical significance based on an FDR correction of $q < 0.05$. While most areas show significant above chance discrimination between different action types for planned actions (red circles), imagined actions (yellow circles) can be accurately predicted from the activity patterns of area aIPS and dPM. In addition, cross-condition classification (orange circles) yields above chance decoding accuracies only in area aIPS, suggesting that the representation of action in this area is independent of the task giving rise to that representation, i.e., imagining an action or planning a real one.

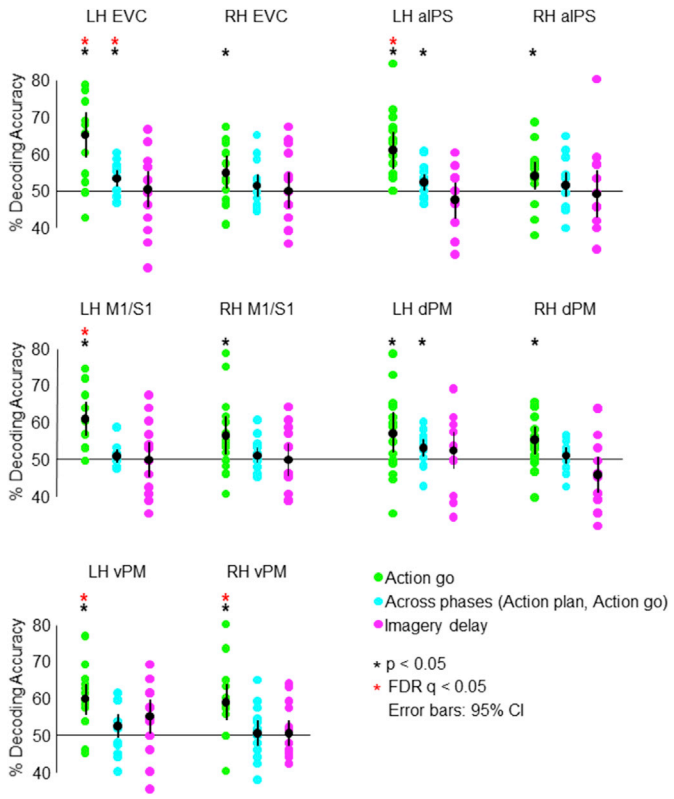

Fig. 7. Classifier decoding accuracies in all ROIs for control comparisons. The scatterplots show decoding accuracies for each participant along with the average (black circles) in left and right hemisphere ROIs for the dissociation between the three movement types during the go phase of Action trials (green circles), across the plan and go phase in Action trials (light-blue circles) and in the delay phase of Imagery trials (fuchsia circles). Chance level is indicated with a line at 50% of decoding accuracy. Error bars show 95% confidence intervals. Black asterisks indicate statistical significance with two-tailed t-tests across subjects with respect to 50%. Red asterisks indicate statistical significance based on an FDR correction of $q < 0.05$. The classifier can accurately discriminate above chance level different action types based on activity patterns elicited during action planning (green circles) in most areas. In addition, cross-phase classification based on activity patterns during action planning and execution (light-blue circles) is significant in the EVC, where cross-condition classification was not possible (see Fig. 6), suggesting that the lack of above chance cross-condition classification accuracy cannot be entirely explained by training and testing the classifier on different phases of the trial.

4. Discussion

The human brain network implicated in hand actions is known to involve a broad range of areas spanning dorsal and ventral visual streams (Gallivan and Culham, 2015; Monaco et al., 2016; Turella and Lingnau, 2014). Recently, there has been a growing interest in the role of V1 during action planning (Gallivan et al., 2019; Gutteling et al., 2015), which has motivated our question about the relation between action planning and motor imagery. Specifically, we asked whether motor imagery and action planning can be dissociated based on the fMRI activity pattern of the EVC, as well as other regions in the frontal and parietal cortex. Further, we examined whether the representation of action is generalized between planned and imagined movements. Our results show that patterns of activity in the EVC allow dissociating between different motor imagery contents, as well as between different motor intentions preceding real movements. However, the representation of planned actions in the EVC differs from the one of imagined actions. Therefore, unlike perception and visual imagery which share a common internal representation in the EVC (Albers et al., 2013), action planning and motor imagery engage overlapping but different neural mechanisms in the visual cortex. While dPM results are similar to EVC, area aIPS, known to be highly specialized in hand movement goals and their abstract representation (Gallivan et al., 2013; Turella et al., 2019), shows that action content can be generalized across imagining movements and planning real actions. The lack of a generalized representation of action in the EVC and dPM, but not in the aIPS might be explained by differences in level of awareness and working-memory components between motor imagery and action intention, and the degree of specialization of visual, parietal and premotor brain areas in processing such components.

During the fMRI session, we measured participants' reaction and movement times to examine whether differences in activity patterns elicited by different movements could be explained by behavioural differences. Indeed, behavioural results showed that both RTs and MTs were significant longer for grasp than reach actions. As for RTs, this difference is likely due to the slightly higher load of information that needs to be processed when planning grasping actions, which require computing object properties (such as size and shape) and the landing position of our digits on the object, as compared to reaching movements, which do not require such detailed information. As for MTs, longer movement durations for grasping than reaching actions might be related to shaping the hand according to object size and task requirements, and this information

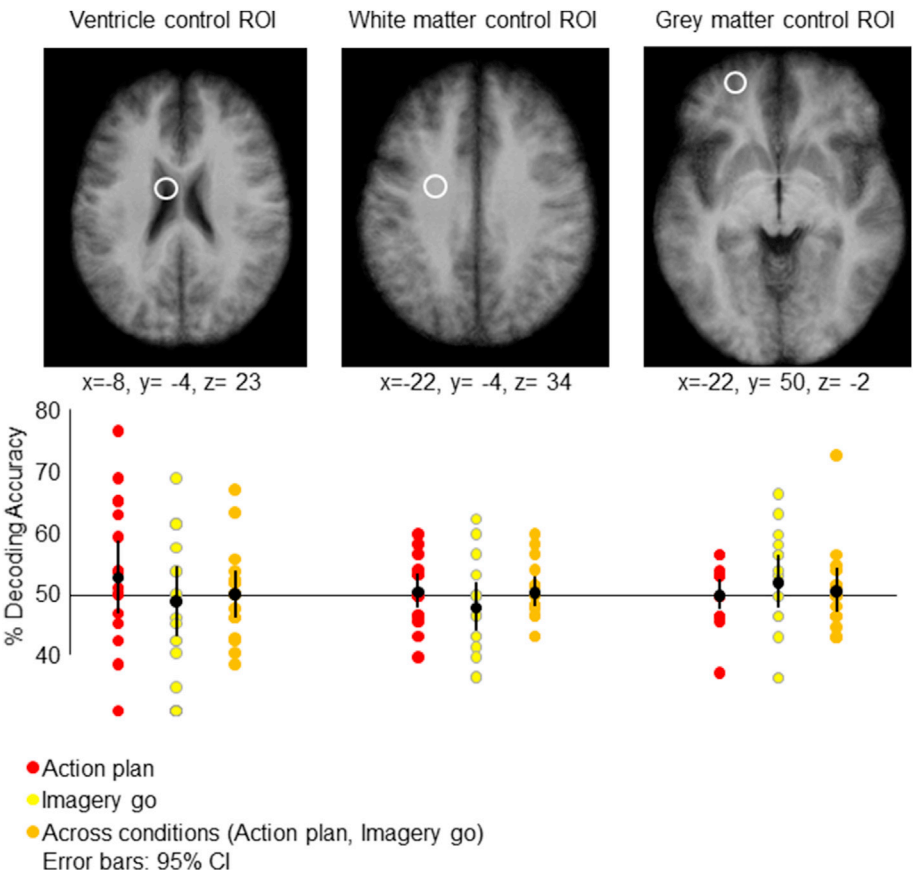

Fig. 8. Classifier decoding accuracies in control regions show no significant decoding accuracy. Three ROIs were defined as control regions to test our classifier in the left ventricle (left panel), white matter (central panel) and grey matter in orbital gyrus (right panel). The scatterplots (lower panel) show decoding accuracies for each participant along with the average (black circles) in the control ROIs for the dissociation between the three movement types during the planning phase of Action trials (red circles), the go phase of Imagery trials (yellow circles) and across Action plan and Imagery go (orange circles). Chance level is indicated with a line at 50% of decoding accuracy. Error bars show 95% confidence intervals. The x, y and z values indicate the Talairach coordinates of each control ROI. Importantly, no significant decoding accuracies were found with respect to 50% chance.

needs to be updated online during movement execution more so for grasping than reaching movements. It is important to note that differences in brain activity patterns between action types during the execution phase of the movement might reflect these behavioural differences. As such, we focused the discussion of our results on the Action plan rather than the Action go phase.

4.1. Early visual cortex

A rich body of neuroimaging studies have shown that mental imagery tasks, in absence of sensory inputs, recruit a network of brain regions that is similar to the one involved in processing incoming information during the real execution of the same tasks. Specifically, visual, tactile, auditory and motor imagery tasks rely on similar neural substrates as those used for visual perception, touch, hearing and movement execution, respectively. Most studies on mental imagery have focused on the primary sensory cortex tied to the type of imagery task (i.e., visual imagery: Ganis et al., 2004; tactile imagery: Yoo et al., 2003; auditory imagery: Yoo et al., 2001; motor imagery: Sharma et al., 2008). As such, the primary visual cortex has been mostly investigated in the context of visual imagery. However, recent evidence and our current results point to a role of V1 that goes beyond visual processing (Gallivan et al., 2019; Gutteling et al., 2015; Monaco et al., 2017; Roelfsema and De Lange, 2016; Snow et al., 2013; Styrkowiec et al., 2019; Vetter et al., 2014) into higher-level cognitive and action-related processes. These studies reinforce the notion that the occipital cortex is involved in action not only in blind individuals, due to intra-modal plasticity processes (Fiehler et al., 2009), but also in sighted ones.

Our findings are the first to demonstrate that inducing motor imagery, as well as action planning, allows decoding of action content in the EVC, despite the fact that activation level as measured with univariate analysis is around baseline level during the motor imagery task. These results cannot be explained in terms of differences in retinal inputs, but likely by predictive coding mechanisms, which are crucial during movement preparation as they allow distinguishing upcoming sensory consequences of our action from external factors, error detection, and quick movement adjustments according to unexpected and sudden changes in the environment. These mechanisms are necessary considering the unavoidable delays of incoming inputs in our sensory system, and motor imagery might allow rehearsing visual anticipations in the EVC through top-down mechanisms.

Note that despite the moderate classification accuracies in the EVC for planned actions, our experiment replicates the results of previous studies showing successful pre-movement decoding in early visual areas (Gallivan et al., 2019; Gutteling et al., 2015), demonstrating a proof of concept and the consistencies of these results across different studies, methods and laboratories. Note that action types could be discriminated based on their activity patterns although univariate analysis showed comparable % signal changes for the three movement types.

Although the finding of motor related aspects in the early visual cortex might seem unexpected, it fits with the idea that the sensory, cognitive and motor domains are strongly interdependent and affect each other even from a neural perspective. In fact, these domains need to interact in order to build predictions and produce appropriate outcomes. A seminal neurophysiology study in primates by Graziano and colleagues (Graziano et al., 1997) demonstrated the presence of bimodal visual and tactile neurons in the ventral premotor cortex, typically known to be involved in motor control. Similarly, a more recent neuroimaging study in humans has shown accurate decoding of images of graspable objects in the primary somatosensory cortex (Smith and Goodale, 2015). The presence of motor-related aspects in the EVC is in line with the idea that sensory and motor information are not processed in isolation and in a limited number of specialized areas, but rather trigger a cascade of events that affects also those areas known to be specialized in other domains or

senses. This process is likely aimed to build predictions, as in a forward model, that take into account as many information (and senses) as possible for the best possible outcome.

While we could successfully decode motor imagery and action planning in the EVC, their content is not shared in this region, as shown by the non-significant cross-condition decoding accuracy. This might be related to the working memory component, which might have been stronger when imagining than planning an action. Indeed, mental imagery has been shown to rely on the same neural codes as working memory tasks (Albers et al., 2013). Another possibility might be related to the different information driving the two tasks, which might have been more visual in nature for motor imagery than for action planning. A third non-mutually exclusive explanation is that action planning and motor imagery entail different levels of awareness, especially for simple movements (see Table 1 in Jeannerod, 2001). For instance, while we purposefully imagine a movement by thinking about it, we are almost unaware while planning our everyday movements. In fact, blindsight patients with primary visual cortex lesions can accurately perform a motor task towards visual stimuli despite not being aware of perceiving these stimuli (Weiskrantz et al., 1974). In short, imagery is a voluntary process while action planning might not be. Yet, one might argue that also imagery can be involuntary, for example when triggered by an association. In our experiment, the auditory instruction at the beginning of the trial might have triggered the mental representation of the action despite participants were asked to wait until the "go" cue at the end of the trial. Thus, we examined whether we could dissociate motor imagery contents during the Imagery delay after the auditory instruction (Fig. 7, fuchsia plots), when action imagery might have been involuntarily triggered by the cue at the beginning of the trial. This analysis did not identify dissociable activity patterns for imagined actions in the EVC (or in any of our ROIs) during the Imagery delay, suggesting that while involuntary motor imagery processes might have taken place during this phase of the trial, they do not seem to be represented in the EVC. In sum, motor imagery in the EVC is detected during voluntary imagery tasks, and the underlying neural mechanisms differ from those of motor planning.

4.2. Parietal and frontal cortices

The evidence of a shared representation of action in the aIPS that can be generalized across real and imagined movements is consistent with previous studies that found cross-condition decoding between action execution and motor imagery in this area (Oosterhof et al., 2012; Zabicki et al., 2017). Importantly, our results extend previous findings by showing that motor imagery in the aIPS can be predicted based on activity patterns during action planning, and vice versa. Among our ROIs, the aIPS showed the most robust cross-condition decoding accuracy, and this result might be explained by the fact that the aIPS is known to be highly specialized in hand actions. This suggests that imagery content is best generalized across tasks (imagining and planning actions) in areas that have an abstract representation of the goal regardless of the task used to achieve the goal, and that are highly specialized in processing the information of the task. In support of this view, the fusiform face area and parahippocampal place area in the ventral visual stream show selective involvement in mental imagery of faces and places, respectively (Craven and Kanwisher, 2000). Taken together, these findings offer evidence that, as for perception, content-specific representations of mental imagery for action, is not only possible in areas specialized in processing specific movement types, but is also shared across imagining and planning the real task. The similarities in the activity patterns of these tasks in the aIPS might allow for effective rehearsal of movements just by imagining them, a process that has been shown to improve motor learning and rehabilitation.

A comparison of the outcome between univariate and multivariate results shows no relation between the involvement of an area in a task, as indicated by univariate activation, and the accurate classification of the task based on the activity pattern. Indeed, while all parietal and frontal areas explored here showed above baseline activation for imagery tasks, only two of them (aIPS and dPM) showed accurate classification. Similarly, despite the lack of above baseline activation for action planning in most frontal and parietal regions of interest (except for left dPM and vPM), action types could be accurately discriminated with multivariate analyses. This reinforces the notion that univariate and multivariate analysis provide complementary and not necessarily equivalent information, with MVPA being more sensitive to distributed representation of information and univariate analysis showing more sensitivity to the overall engagement in a task (Coutanche, 2013; Davis et al., 2014; Jimura and Poldrack, 2012).

One surprising aspect of our results is the weak cross-condition decoding accuracy in premotor areas. Indeed, planning an action as well as forming a mental image of an action have been shown to involve activity in frontal areas (Gallivan et al., 2011; Ranganath and D'Esposito, 2005). Consistent with this, the activity patterns in dPM reflect imagined or upcoming action, but they only weakly allow generalizing across the two tasks. Our finding reinforces the idea that the degree of content-similarity (action type) across task modalities (plan or imagine) is strongly dependent on the degree of specialization of a brain area in processing that particular content (such as the aIPS for grasping actions). A model of visual imagery dynamics has been recently put forward by Pearson (2019), and suggests a visual hierarchy trend according to which patterns of activity that are common to perception and visual imagery arise as early as V1 and become increasingly similar in higher level visual areas in the ventral stream, where visual imagery content have more perception-like representations. This trend seems to be reflected also in the motor domain, where action representation is generalized across planning and imagining actions in higher level areas in the action network, such as the aIPS, and becomes weaker in areas that are anatomically distant from the aIPS, like premotor areas, where cross-decoding was weak or absent.

Motor imagery and action planning share representations of content in parietal but not premotor cortex, and this is in line with findings showing that electrical stimulation of parietal cortex evoked conscious intention and motor awareness (the awareness that we are actually executing a movement) without any motor output. In contrast, stimulation of the premotor cortex induced real movements, without motor awareness (Desmurget et al., 2009). Therefore, the awareness required during motor imagery tasks might be one of the components that characterizes the cross-decoding between action intentions and motor imagery in the posterior parietal cortex, suggesting that here the power of motor imagery is comparable to the willingness to move (Aflalo et al., 2015), and is then transformed into a motor output only at a later stage in more anterior premotor and motor regions.

Motor imagery has important applications in the field of brain computer interfaces (BCI) that enable direct communication between the brain and computers. The growing interest in BCI in the neuroscientific realm is related to the employment of this technique as a medical source of support for individuals with neuromuscular disorders, spinal injuries, or limited mobility in the extremities. While the motor component is fundamental for the generation of a movement, sensory predictions play an important role for motor planning. The identification of brain areas, in addition to the primary motor cortex, that consistently represent imagined actions, and whose representation resembles the one of motor planning, will help with the selection of cortical areas to be targeted for the use of brain-computer interfaces that allow controlling effectors by imagining the desired movement. In this study, we directly compared classification outputs of intended and imagined actions, and showed that their neural representation spans from occipital to frontal regions. However, only the anterior intraparietal area shows similar representations between intended and imagined actions, and might represent the ideal candidate for controlling external devices through motor imagery tasks.

While visual attention might have played a role in the performance of our task, the different task-related demands might not be reflected in the

MVPA results. In fact, MVPA is more sensitive to distributed representation of information related to task identity rather than the overall engagement in a task (Jimura and Poldrack, 2012). As such, although different actions require processing different aspects of the object or the visual scene by engaging attentional mechanisms, these might differentially affect the univariate results more than the MVPA results. Indeed, attentional load has been shown to affect the strength of task-related activity, as measured with univariate analysis, but not the representation of task identity indicated by MVPA (Chan et al., 2015).

4.3. Limitations of the study

We assessed motor imagery vividness with the VMIQ-2 to ensure that our participants had good imagery ability, which would have been reflected in the motor imagery task during the scan session. The lack of significant correlations between subjective vividness ratings and % signal change or decoding accuracies extracted from imagery trials might appear to be in contrast with previous findings showing that the amplitude of the neural activity as well as neural activation patterns during motor imagery tasks relate to the individual vividness of imagined actions (Zabicki et al., 2019). However, while in these studies the vividness rating referred to the action that was imagined during the fMRI task (and the response was recorded during the scan session immediately after the imagery trial), in our experiment the actions imagined for the questionnaire and the scan session differed. Therefore, lack of significant correlations in this study is likely related to the fact that the actions that participants imagined for the questionnaire differed significantly form the ones imagined during the scan sessions, and the activity patterns for the fMRI session were specifically discriminated based on action types.

5. Conclusions

To conclude, our findings show that motor intentions and motor imagery have overlapping neural representations spanning premotor to visual cortices in areas dPM, aIPS and EVC. While the encoding of action planning in the EVC is in agreement with recent neuroimaging findings (Gallivan et al., 2019), we are not aware of any investigation of neural decoding of motor imagery in the visual cortex, and its relation to motor intention. We found that despite the overlap in parietal, frontal and early visual cortex, only the aIPS has a shared representation of actions that generalizes between imagining actions and planning real movements.

Data availability statement

Codes used for the analysis are publicly available at http://cosmomvpa.org (Oosterhof et al., 2016). Data will be made available from the authors to anyone who wishes to replicate our findings or investigate other aspects related to our paradigm. To request the data, send an email to simona.monaco@gmail.com.

Declaration of competing interest

The authors declare no competing financial interests.

Funding

This project has received funding from the European Union's Horizon 2020 research and innovation programme under the Marie Sklodowska-Curie grant agreement No 703597, and the European Research Council (ERC) grant agreement No 339939.

CRediT authorship contribution statement

Simona Monaco: Conceptualization, Methodology, Software, Validation, Formal analysis, Investigation, Writing - original draft, Visualization, Supervision, Project administration, Funding acquisition. **Giulia Malfatti:** Investigation, Writing - review & editing. **Jody C. Culham:** Writing - review & editing. **Luigi Cattaneo:** Writing - review & editing. **Luca Turella:** Conceptualization, Methodology, Resources, Software, Writing - review & editing, Supervision, Project administration, Funding acquisition.

Acknowledgements

The authors are thankful to Claudio Boninsegna, Manuela Orsini, and Pietro Chiesa for technical support; Enrica Pierotti and Flavio Ragni for help with eye-tracking data acquisition and analyses; our participants.

References

Aflalo, T., Kellis, S., Klaes, C., Lee, B., Shi, Y., Pejsa, K., Shanfield, K., Hayes-Jackson, S., Aisen, M., Heck, C., Liu, C., Andersen, R.A., 2015. Decoding motor imagery from the posterior parietal cortex of a tetraplegic human. Science 84 348, 906–910. https://doi.org/10.1126/science.aaa5417.

Aggarwal, S., Chugh, N., 2019. Signal processing techniques for motor imagery brain computer interface: a review. Array 1 (2). https://doi.org/10.1016/j.array.2019.100003, 100003.

Albers, A.M., Kok, P., Toni, I., Dijkerman, H.C., de Lange, F.P., 2013. Shared representations for working memory and mental imagery in early visual cortex. Curr. Biol. 23, 1427–1431. https://doi.org/10.1016/J.CUB.2013.05.065.

Annett, J., 1995. Motor imagery: perception or action? Neuropsychologia 33, 1395–1417. https://doi.org/10.1016/0028-3932(95)00072-B.

Ariani, G., Wurm, M.F., Lingnau, a., 2015. Decoding internally and externally driven movement plans. J. Neurosci. 35, 14160–14171. https://doi.org/10.1523/JNEUROSCI.0596-15.2015.

Batula, A.M., Mark, J.A., Kim, Y.E., Ayaz, H., 2017. Comparison of brain activation during motor imagery and motor movement using fNIRS. Comput. Intell. Neurosci. https://doi.org/10.1155/2017/5491296, 2017.

Bechara, A., 2004. Disturbances of emotion regulation after focal brain lesions. Int. Rev. Neurobiol. https://doi.org/10.1016/S0074-7742(04)62006-X.

Benjamini, Y., Yekutieli, D., 2001. The control of the False Discovery rate in multiple testing under dependency. Ann. Stat. https://doi.org/10.2307/2674075.

Bruno, V., Fossataro, C., Garbarini, F., 2018. Inhibition or facilitation? Modulation of corticospinal excitability during motor imagery. Neuropsychologia 111, 360–368. https://doi.org/10.1016/j.neuropsychologia.2018.02.020.

Chan, J.L., Kucyi, A., Desouza, J.F.X., 2015. Stable task representations under attentional load revealed with multivariate pattern analysis of human brain activity. J. Cognit. Neurosci. https://doi.org/10.1162/jocn_a_00819, 2015.

Chen, W., Kato, T., Zhu, X.-H., Ogawa, S., Tank, D.W., Ugurbil, K., 1998. Human primary visual cortex and lateral geniculate nucleus activation during visual imagery. Neuroreport 9, 3669–3674. https://doi.org/10.1097/00001756-199811160-00019.

Coutanche, M.N., 2013. Distinguishing multi-voxel patterns and mean activation: why, how, and what does it tell us? Cognit. Affect Behav. Neurosci. 13, 667–673. https://doi.org/10.3758/s13415-013-0186-2.

Craven, K.M.O., Kanwisher, N., 2000. Mental imagery of faces and places activates corresponding stimulus-specific brain regions. J. Cognit. Neurosci. 12, 1013–1023.

Culham, J.C., Danckert, S.L., DeSouza, J.F.X., Gati, J.S., Menon, R.S., Goodale, M.A., 2003. Visually guided grasping produces fMRI activation in dorsal but not ventral stream brain areas. Exp. Brain Res. 153, 180–189.

Davis, T., LaRocque, K.F., Mumford, J.A., Norman, K.A., Wagner, A.D., Poldrack, R.A., 2014. What do differences between multi-voxel and univariate analysis mean? How subject-, voxel-, and trial-level variance impact fMRI analysis. Neuroimage. https://doi.org/10.1016/j.neuroimage.2014.04.037.

Desmurget, M., Reilly, K.T., Richard, N., Szathmari, A., Mottolese, C., Sirigu, A., 2009. Movement intention after parietal cortex stimulation in humans. Science 84 324, 811–813. https://doi.org/10.1126/science.1169896.

D'Esposito, M., Detre, J.A., Aguirre, G.K., Stallcup, M., Alsop, D.C., Tippet, L.J., Farah, M.J., 1997. A functional MRI study of mental image generation. Neuropsychologia. https://doi.org/10.1016/S0028-3932(96)00121-2.

Dijkstra, N., Bosch, S.E., van Gerven, M.A.J., 2017. Vividness of visual imagery depends on the neural overlap with perception in visual areas. J. Neurosci. 37, 1367–1373. https://doi.org/10.1523/JNEUROSCI.3022-16.2016.

Doyon, J., Penhune, V., Ungerleider, L.G., 2003. Distinct contribution of the cortico-striatal and cortico-cerebellar systems to motor skill learning. Neuropsychologia 41, 252–262. https://doi.org/10.1016/S0028-3932(02)00158-6.

Ehrsson, H.H., Geyer, S., Naito, E., 2003. Imagery of voluntary movement of fingers, toes, and tongue activates corresponding body-part-specific motor representations. J. Neurophysiol. 90, 3304–3316. https://doi.org/10.1152/jn.01113.2002.

Fiehler, K., Burke, M., Bien, S., Röder, B., Rösler, F., 2009. The human dorsal action control system develops in the absence of vision. Cerebr. Cortex 19, 1–12. https://doi.org/10.1093/cercor/bhn067.

Formisano, E., Linden, D.E.J., Di Salle, F., Trojano, L., Esposito, F., Sack, A.T., Grossi, D., Zanella, F.E., Goebel, R., 2002. Tracking the mind's image in the brain I: time-resolved fMRI during visuospatial mental imagery. Neuron. https://doi.org/10.1016/S0896-6273(02)00747-X.

Gallivan, J.P., Chapman, C.S., Gale, D.J., Flanagan, J.R., Culham, J.C., 2019. Selective modulation of early visual cortical activity by movement intention. Cerebr. Cortex 1–17. https://doi.org/10.1093/cercor/bhy345.

Gallivan, J.P., Culham, J.C., 2015. Neural coding within human brain areas involved in actions. Curr. Opin. Neurobiol. 33, 141–149. https://doi.org/10.1016/j.conb.2015.03.012.
Gallivan, J.P., Mclean, D.A., Flanagan, J.R., Culham, J.C., 2013. Where one hand meets the other: limb-specific and action- dependent movement plans decoded from preparatory signals in single human frontoparietal brain areas. J. Neurosci. 33 https://doi.org/10.1523/JNEUROSCI.0541-12.2013, 1991–2008.
Gallivan, J.P., Mclean, D.A., Valyear, K.F., Pettypiece, C.E., Culham, J.C., 2011. Decoding action intentions from preparatory brain activity in human parieto-frontal networks. J. Neurosci. 31, 9599–9610. https://doi.org/10.1523/JNEUROSCI.0080-11.2011.
Ganis, G., Thompson, W.L., Kosslyn, S.M., 2004. Brain areas underlying visual mental imagery and visual perception: an fMRI study. Cognit. Brain Res. 20, 226–241. https://doi.org/10.1016/j.cogbrainres.2004.02.012.
Glover, G.H., 1999. Deconvolution of impulse response in event-related BOLD fMRI. Neuroimage. https://doi.org/10.1006/nimg.1998.0419.
Graziano, M.S.A., Hu, X.T., Gross, C.G., 1997. Visuospatial properties of ventral premotor cortex. J. Neurophysiol. 2268–2292.
Green, A.M., Kalaska, J.F., 2011. Learning to move machines with the mind. Trends Neurosci. 34, 61–75. https://doi.org/10.1016/j.tins.2010.11.003.
Guillot, A., Collet, C., Nguyen, V.A., Malouin, F., Richards, C., Doyon, J., 2008. Functional neuroanatomical networks associated with expertise in motor imagery. Neuroimage 41, 1471–1483. https://doi.org/10.1016/j.neuroimage.2008.03.042.
Gutteling, T.P., Petridou, N., Dumoulin, S.O., Harvey, B.M., Aarnoutse, E.J., Kenemans, J.L., Neggers, S.F.W., 2015. Action preparation shapes processing in early visual cortex. J. Neurosci. 35, 6472–6480. https://doi.org/10.1523/JNEUROSCI.1358-14.2015.
Hardwick, R.M., Caspers, S., Eickhoff, S.B., Swinnen, S.P., 2018. Neural correlates of action: comparing meta-analyses of imagery, observation, and execution. Neurosci. Biobehav. Rev. 94, 31–44. https://doi.org/10.1016/J.NEUBIOREV.2018.08.003.
Haynes, J.D., 2015. A primer on pattern-based approaches to fMRI: principles, pitfalls, and perspectives. Neuron. https://doi.org/10.1016/j.neuron.2015.05.025.
Höhne, J., Holz, E., Staiger-Sälzer, P., Müller, K.-R., Kübler, A., Tangermann, M., 2014. Motor imagery for severely motor-impaired patients: evidence for brain-computer interfacing as superior control solution. PLoS One 9, e104854. https://doi.org/10.1371/journal.pone.0104854.
Isaac, A.R., Marks, D.F., 1994. Individual differences in mental imagery experience: developmental changes and specialization. Br. J. Psychol. 85, 479–500. https://doi.org/10.1111/j.2044-8295.1994.tb02536.x.
Ishai, A., Haxby, J.V., Ungerleider, L.G., 2002. Visual imagery of famous faces: effects of memory and attention revealed by fMRI. Neuroimage 17, 1729–1741. https://doi.org/10.1006/nimg.2002.1330.
Jeannerod, M., 2001. Neural simulation of action: a unifying mechanism for motor cognition. In: NeuroImage, pp. 103–109. https://doi.org/10.1006/nimg.2001.0832.
Jeannerod, M., Decety, J., 1995. Mental motor imagery: a window into the representational stages of action. Curr. Opin. Neurobiol. https://doi.org/10.1016/0959-4388(95)80099-9.
Jimura, K., Poldrack, R.A., 2012. Analyses of regional-average activation and multivoxel pattern information tell complementary stories. Neuropsychologia. https://doi.org/10.1016/j.neuropsychologia.2011.11.007.
Kaplan, J.T., Man, K., Greening, S.G., 2015. Multivariate cross-classification: applying machine learning techniques to characterize abstraction in neural representations. Front. Hum. Neurosci. 9, 151. https://doi.org/10.3389/fnhum.2015.00151.
Kilteni, K., Andersson, B.J., Houborg, C., Ehrsson, H.H., 2018. Motor imagery involves predicting the sensory consequences of the imagined movement. Nat. Commun. 9, 1–9. https://doi.org/10.1038/s41467-018-03989-0.
Klein, I., Paradis, A.L., Poline, J.B., Kosslyn, S.M., Le Bihan, D., 2000. Transient activity in the human calcarine cortex during visual-mental imagery: an event-related fMRI study. J. Cogn. Neurosci. 12, 15–23. https://doi.org/10.1162/089892900564037.
Knauff, M., Kassubek, J., Mulack, T., Greenlee, M.W., 2000. Cortical activation evoked by visual mental imagery as measured by fMRI. Neuroreport 11, 3957–3962.
Koenig-Robert, R., Pearson, J., 2019. Decoding the contents and strength of imagery before volitional engagement. Sci. Rep. 9, 1–14. https://doi.org/10.1038/s41598-019-39813-y.
Kriegeskorte, N., Lindquist, M.A., Nichols, T.E., Poldrack, R.A., Vul, E., 2010. Everything you never wanted to know about circular analysis, but were afraid to ask. J. Cerebr. Blood Flow Metabol. 30, 1551–1557. https://doi.org/10.1038/jcbfm.2010.86.
Lambert, S., Sampaio, E., Scheiber, C., Mauss, Y., 2002. Neural substrates of animal mental imagery: calcarine sulcus and dorsal pathway involvement - an fMRI study. Brain Res. https://doi.org/10.1016/S0006-8993(01)03232-2.
Le Bihan, D., Turner, R., Zeffiro, T.A., Cuenod, C.A., Jezzard, P., Bonnerot, V., 1993. Activation of human primary visual cortex during visual recall: a magnetic resonance imaging study. Proc. Natl. Acad. Sci. U. S. A. 90, 11802–11805. https://doi.org/10.1073/pnas.90.24.11802.
Markov, N.T., Misery, P., Falchier, A., Lamy, C., Vezoli, J., Quilodran, R., Gariel, M.A., Giroud, P., Ercsey-Ravasz, M., Pilaz, L.J., Huissoud, C., Barone, P., Dehay, C., Toroczkai, Z., Van Essen, D.C., Kennedy, H., Knoblauch, K., 2011. Weight consistency specifies regularities of macaque cortical networks. Cerebr. Cortex 21, 1254–1272. https://doi.org/10.1093/cercor/bhq201.
Mizuguchi, N., Nakata, H., Kanosue, K., 2016. Motor imagery beyond the motor repertoire: activity in the primary visual cortex during kinesthetic motor imagery of difficult whole body movements. Neuroscience 315, 104–113. https://doi.org/10.1016/j.neuroscience.2015.12.013.
Monaco, S., Buckingham, G., Sperandio, I., Doug Crawford, J., 2016. Editorial: perceiving and acting in the real world: from neural activity to behavior. Front. Hum. Neurosci. 10, 1–4. https://doi.org/10.3389/fnhum.2016.00179.
Monaco, S., Cavina-Pratesi, C., Sedda, A., Fattori, P., Galletti, C., Culhaml, J.C., Culham, J.C., 2011. Functional magnetic resonance adaptation reveals the involvement of the dorsomedial stream in hand orientation for grasping. J. Neurophysiol. 106, 2248–2263. https://doi.org/10.1152/jn.01069.2010.
Monaco, S., Chen, Y., Medendorp, W.P., Crawford, J.D., Fiehler, K., Henriques, D.Y.P., 2014. Functional magnetic resonance imaging adaptation reveals the cortical networks for processing grasp-relevant object properties. Cerebr. Cortex 24. https://doi.org/10.1093/cercor/bht006.
Monaco, S., Gallivan, J.P., Figley, T.D., Singhal, A., Culham, J.C., 2017. Recruitment of foveal retinotopic cortex during haptic exploration of shapes and actions in the dark. J. Neurosci. 37 https://doi.org/10.1523/JNEUROSCI.2428-16.2017, 2428–16.
Monaco, S., Malfatti, G., Zendron, A., Pellencin, E., Turella, L., 2019. Predictive coding of action intentions in dorsal and ventral visual stream is based on visual anticipations, memory-based information and motor preparation. Brain Struct. Funct. https://doi.org/10.1007/s00429-019-01970-1.
Naselaris, T., Olman, C., Stansbury, D., Ugurbil, K., Gallant, J., 2015. A voxel-wise encoding model for early visual areas decodes mental images of remembered scenes. Neuroimage 15, 215–228. https://doi.org/10.1016/j.neuroimage.2014.10.018. https://search.crossref.org/?q=A+voxel-wise+encoding+model+for+early+visual+areas+decodes+mental+images+of+remembered+scenes.
Norman, K.A., Polyn, S.M., Detre, G.J., Haxby, J.V., 2006. Beyond mind-reading: multi-voxel pattern analysis of fMRI data. Trends Cognit. Sci. 10, 424–430. https://doi.org/10.1016/j.tics.2006.07.005.
Nyberg, L., Eriksson, J., Larsson, A., Marklund, P., 2006. Learning by doing versus learning by thinking: an fMRI study of motor and mental training. Neuropsychologia 44, 711–717. https://doi.org/10.1016/j.neuropsychologia.2005.08.006.
Ogawa, S., Tank, D., Menon, R.S., Ellermann, J.M., Kim, S.G., Merkle, H., Ugurbil, K., 1992. Intrinsic signal changes accompanying sensory stimulation: functional brain mapping with magnetic resonance imaging. Proc. Natl. Acad. Sci. Unit. States Am. 89, 5951–5955. https://doi.org/10.1016/S0006-3495(93)81441-3.
Oosterhof, N.N., Connolly, A.C., Haxby, J.V., 2016. CoSMoMVPA: multi-modal multivariate pattern analysis of neuroimaging data in matlab/GNU octave. Front. Neuroinf. 10 https://doi.org/10.3389/fninf.2016.00027.
Oosterhof, N.N., Tipper, S.P., Downing, P.E., 2012. Visuo-motor imagery of specific manual actions: a multi-variate pattern analysis fMRI study. Neuroimage 63, 262–271. https://doi.org/10.1016/J.NEUROIMAGE.2012.06.045.
Page, S.J., Levine, P., Leonard, A., 2007. Mental practice in chronic stroke: Results of a randomized, placebo-controlled trial. Stroke 38, 1293–1297. https://doi.org/10.1161/01.STR.0000260205.67348.2b.
Pearson, J., 2019. The human imagination: the cognitive neuroscience of visual mental imagery. Nat. Rev. Neurosci. 20, 624–634. https://doi.org/10.1038/s41583-019-0202-9.
Pearson, J., Naselaris, T., Holmes, E.A., Kosslyn, S.M., 2015. Mental imagery: functional mechanisms and clinical applications. Trends Cognit. Sci. 19, 590–602. https://doi.org/10.1016/j.tics.2015.08.003.
Pearson, J., Westbrook, F., 2015. Phantom perception: voluntary and involuntary nonretinal vision. Trends Cognit. Sci. 19, 278–284. https://doi.org/10.1016/j.tics.2015.03.004.
Ranganath, C., D'Esposito, M., 2005. Directing the mind's eye: prefrontal, inferior and medial temporal mechanisms for visual working memory. Curr. Opin. Neurobiol. https://doi.org/10.1016/j.conb.2005.03.017.
Roberts, R., Callow, N., Hardy, L., Markland, D., Bringer, J., 2008. Movement imagery ability: development and assessment of a revised version of the vividness of movement imagery questionnaire. J. Sport Exerc. Psychol.
Roelfsema, P.R., De Lange, F.P., 2016. Early Visual Cortex as a Multiscale Cognitive Blackboard. https://doi.org/10.1146/annurev-vision-111815-114443.
Sabbah, P., Simond, G., Levrier, O., Habib, M., Trabaud, V., Murayama, N., Mazoyer, B.M., Briant, J.F., Raybaud, C., Salamon, G., 1995. Functional magnetic resonance imaging at 1.5 T during sensorimotor and cognitive task. Eur. Neurol. 35, 131–136. https://doi.org/10.1159/000117108.
Sharma, N., Jones, P.S., Carpenter, T.A., Baron, J.C., 2008. Mapping the involvement of BA 4a and 4p during motor imagery. Neuroimage. https://doi.org/10.1016/j.neuroimage.2008.02.009.
Shepherd, G.M., 2007. Perspectives on olfactory processing, conscious perception, and orbitofrontal cortex. In: Annals of the New York Academy of Sciences. Blackwell Publishing Inc., pp. 87–101. https://doi.org/10.1196/annals.1401.032
Singhal, A., Monaco, S., Kaufman, L.D., Culham, J.C., Jacobs, C., 2013. Human fMRI reveals that delayed action Re-recruits visual perception. PLoS One 8, e73629. https://doi.org/10.1371/journal.pone.0073629.
Smith, F.W., Goodale, M.A., 2015. Decoding visual object categories in early somatosensory cortex. Cerebr. Cortex 25, 1020–1031. https://doi.org/10.1093/cercor/bht292.
Snow, J.C., Strother, L., Humphreys, G.W., 2013. Haptic shape processing in visual cortex. J. Cognit. Neurosci. 26, 194–198. https://doi.org/10.1162/jocn.
Styrkowiec, P.P., Nowik, A.M., Króliczak, G., 2019. The neural underpinnings of haptically guided functional grasping of tools: an fMRI study. Neuroimage. https://doi.org/10.1016/j.neuroimage.2019.03.043.
Swisher, J.D., Halko, M.A., Merabet, L.B., McMains, S.A., Somers, D.C., 2007. Topography of human intraparietal sulcus. J. Neurosci. 27, 5326–5337. https://doi.org/10.1523/JNEUROSCI.0991-07.2007.
Talairach, J., Tournoux, P., 1988. Co-planar Stereotaxic Atlas of the Human Brain. Theime, New York.
Trojano, L., Grossi, D., Linden, D., Formisano, E., Hacker, H., Zanella, F., Goebel, R., di Salle, F., 2000. Matching two imagined clocks: the functional anatomy of spatial analysis in the absence of visual stimulation. Cerebr. Cortex 10, 473–481. https://doi.org/10.1093/cercor/10.5.473.

Turella, L., Lingnau, A., 2014. Neural correlates of grasping. Front. Hum. Neurosci. 8, 686. https://doi.org/10.3389/fnhum.2014.00686.

Turella, L., Rumiati, R., Lingnau, A., 2019. Hierarchical action encoding within the human brain. Cerebr. Cortex (in press).

Vetter, P., Smith, F.W., Muckli, L., 2014. Decoding sound and imagery content in early visual cortex. Curr. Biol. 24, 1256–1262.

Vul, E., Kanwisher, N., Kanwisher, Nancy, 2010. Begging the question: the nonindependence error in fMRI data analysis. In: Hanson, S., Bunzl, M. (Eds.), Foundational Issues for Human Brain Mapping. The MIT Press, MIT Press, Cambridge, MA, pp. 71–91. https://doi.org/10.7551/mitpress/9780262014021.003.0007.

Weiskrantz, L., Warrington, E., Sanders, M., Marshall, J., 1974. Visual capacity in the hemianopic field following a restricted occipital ablation. Brain 97, 709–728. https://doi.org/10.1093/brain/97.1.709.

Zabicki, A., de Haas, B., Zentgraf, K., Stark, R., Munzert, J., Krüger, B., 2019. Subjective vividness of motor imagery has a neural signature in human premotor and parietal cortex. Neuroimage 197, 273–283. https://doi.org/10.1016/j.neuroimage.2019.04.073.

Wheeler, M.E., Petersen, S.E., 2000. Memory's echo: vivid remembering reactivates sensory-specific cortex. Proc. Natl. Acad. Sci. 97, 11125–11129.

Yoo, S.-S., Freeman, D.K., McCarthy, J.J., Jolesz, F.A., 2003. Neural substrates of tactile imagery: a functional MRI study. Neuroreport 14, 581–585. https://doi.org/10.1097/00001756-200303240-00011.

Yoo, S.-S., Lee, C.U., Choi, B.G., 2001. Human brain mapping of auditory imagery: event-related functional MRI study. Neuroreport 12, 3045–3049. https://doi.org/10.1097/00001756-200110080-00013.

Zabicki, A., De Haas, B., Zentgraf, K., Stark, R., Munzert, J., Krüger, B., 2017. Imagined and executed actions in the human motor system: testing neural similarity between execution and imagery of actions with a multivariate approach. Cerebr. Cortex 27, 4523–4536. https://doi.org/10.1093/cercor/bhw257.